



## Mapping inundation of estuarine margins driven by ocean and fluvial forcings

André B. FORTUNATO<sup>1</sup>, Paula FREIRE<sup>1</sup>, Ana RILO<sup>1</sup>, Teresa VISEU<sup>1</sup>, Marta RODRIGUES<sup>1</sup>

<sup>1</sup> National Laboratory for Civil Engineering, Portugal  
{afortunato, pfreire, arilo, tviseu, mfrodrigues}@lnec.pt

### ABSTRACT

Inundation maps are required for spatial planning. This paper describes the generation of inundation maps for the margins of the upstream region of the Tagus estuary (Portugal). Maps are constructed separately for a major river flood (the February 1979 flood) and an extreme storm surge (the February 1941 cyclone), both with return periods on the order of 100 years. All the relevant forcings are considered in the model simulations, including tides, river flow, wind, atmospheric pressure and surface waves. The dykes that protect the margins are explicitly considered by placing a row of grid nodes along their crests. The impact of sea level rise is also assessed.

### 1. Introduction

Spatial planning for territories located on the margins of water bodies requires maps of inundation for both present and future conditions. Estuarine margins are a peculiar case, as they can be inundated by both oceanic phenomena, namely spring tides combined with storm surges, or river floods. The dominant cause of inundation varies spatially: river floods dominate in the upper estuary, while floods of oceanic origin prevail downstream. Additionally, both river floods and storms usually coincide with adverse meteorological conditions. As a result, many extreme events are influenced by both river and ocean forces (compound flooding). Developing inundation maps for estuarine margins is therefore a complicated task, which implies considering a wide diversity of physical processes and spatial scales.

The generation of inundation maps in estuarine margins is illustrated here for the Tagus Estuary. The Tagus Estuary, located on the Portuguese west coast (Fig. 1), covers approximately 320 km<sup>2</sup>. It features a deep, long, and narrow tidal inlet connecting the Atlantic Ocean to a wide, shallow, tide-dominated basin with extensive tidal flats and salt marshes, encompassing about 40% of the inner estuary surface. About 40 km upstream, the estuary markedly narrows at the bay head. Tidal ranges vary between 0.55 and 3.86 m in the open coast (Guerreiro et al., 2015) but resonance significantly amplifies the semi-diurnal tidal constituents within the estuary (Fortunato et al., 1999). Simultaneously, the estuary is strongly ebb-dominated due to the large extent of the tidal flats (Fortunato et al., 1999). The average river flow of the Tagus is about 300 m<sup>3</sup>/s. However, the peak river flow can exceed 10,000 m<sup>3</sup>/s during large floods. The Tagus is also exposed to large waves coming from the Atlantic Ocean. Fortunato et al. (2017) estimated significant wave heights of 13-14 m during a major storm.

This paper focuses on the upstream reaches of the Tagus Estuary, particularly in the Vila Franca de Xira municipality. In this part of the estuary, there are extensive marginal areas with very low elevations. Many of these areas are protected by dykes to prevent frequent flooding. Land uses in these margins include agriculture, urban development and industry.

This paper is organized as follows. Section 2 describes the methods followed, including the approach, the choice of the events to simulate, and the model used. The results are presented and discussed in Section 3. The paper closes with a summary of the lessons learned to inform future similar studies.

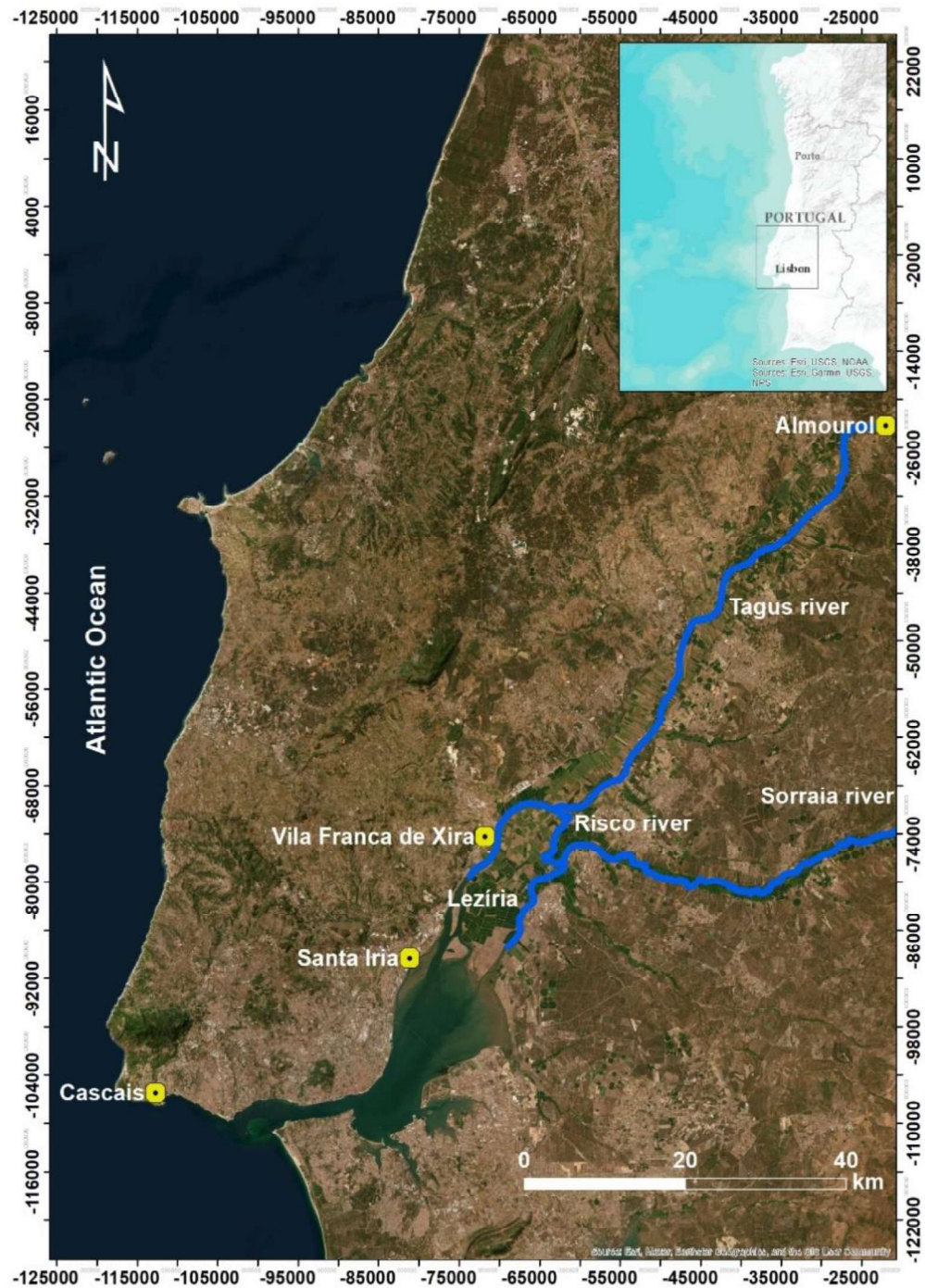


Fig. 1. The Tagus Estuary: location and place names (credits: ArcGIS® Online Base Maps)

## 2. Methods

### 2.1. General approach

The margins of the Tagus estuary can be inundated due to oceanic phenomena (high tides combined with storm surges) or to fluvial phenomena (flood flows). The dominant cause varies spatially, with river floods dominating upstream and oceanic floods prevailing downstream. In the Vila Franca de Xira municipality, at the Tagus estuary's upstream limit, both causes can be significant. Oceanic floods might dominate the south, while fluvial floods might be more prominent in the north. The exact transition zone remains to be determined. Additionally, a positive correlation between extreme river flows and major storm surges is expected, highlighting the need to consider both river and ocean influences when assessing extreme water levels.

The SCHISM numerical model (Zhang et al., 2016) simulates water levels and currents in the Tagus Estuary, considering tides, river flow, wind, atmospheric pressure, and wave action. Encompassing the entire estuary and potentially floodable areas in Vila Franca de Xira, the model simulates 100-year return period oceanic and fluvial flood events with realistic atmospheric, oceanographic, and riverine drivers. Atmospheric drivers were obtained from the 20<sup>th</sup> Century Reanalysis or from ERA5 (Hersbach et al., 2020). Waves at the model boundary were obtained from implementations of the model WaveWatch III to the North Atlantic (Fortunato et al., 2017). The final flood maps combine information from both simulations.

Inundation maps were generated for two events with return periods of the order of 100 years: the February 1941 cyclone, and the February 1979 river flood.

## 2.2. Extreme events

Unlike fluvial floods with a single dominant driver, oceanic floods involve a complex interplay of tides, storm surges, wave setup, and river flow. Each phenomenon contributes to water levels along the estuary in unique ways, with some propagating upstream, some downstream, and others generated locally. As a result, the same event can lead to water levels with different return periods along the estuary. For instance, a southerly wind during a storm will raise water levels on the north bank and lower them on the south bank. Consequently, the return period of the highest water levels during such an event will be higher on the north bank compared to the south. Hence, in the case of floods of maritime origin, a return period should not be assigned to an event, strictly speaking.

Therefore, to assess oceanic flooding, we simulated the hydrodynamics in the Tagus Estuary for the most severe 20<sup>th</sup>-century event: the 1941 cyclone. This cyclone caused widespread flooding and casualties throughout the Tagus estuary (Muir-Wood, 2011; Freitas and Dias, 2013). According to Fortunato et al. (2017), the tidal range corresponds only to the 91<sup>st</sup> percentile of tides; the wave surge had a return period of over 100 years; the sea levels in Cascais corresponded to a return period of 20 years; the river flow corresponded to a return period of 3 years; and the atmospheric pressure had a return period probably greater than 65 years. Overall, the return period of water levels inside the estuary associated with an event of this magnitude is of the order of 100 years, so the event is suitable for delimiting the area threatened by floods for a return period of 100 years.

Atmospheric conditions for the 1941 event were provided by an application of the model WRF-ARW forced by the 20<sup>th</sup> Century Reanalysis (20CRv2). These conditions were also used to force the wave model WW3 in the North Atlantic to provide the wave boundary conditions for the estuarine model (Fortunato et al., 2017). Atmospheric pressure, offshore significant wave height ( $H_s$ ) and river flow reached 952 hPa, 14 m and 4500 m<sup>3</sup>/s, respectively. The river flow, estimated from measurements from the Vila Velha de Rodão monitoring station, reached about 1000 m<sup>3</sup>/s during the peak of the storm. Simulations were performed for both the present mean sea level (MSL) and assuming 1.5 m sea level rise. The present MSL was obtained by analyzing elevation data from the Cascais tide gauge since the late 19<sup>th</sup> century (Fig. 2). According to these data, MSL has risen by 20 cm since Portuguese vertical datum was defined in 1938. The future sea level rise, 1.5 m, is the one recommended by the Portuguese Environmental Protection Agency. This value can be considered a prudent assumption, given the most recent projections of the International Panel on Climate Change for the end of the 21<sup>st</sup> century.

The February 1979 flood was the largest flood of the River Tagus in the 20<sup>th</sup> century, in terms of both water levels reached and destruction in Santarém and the lower Tagus valley, affecting the water supply to Lisbon. The flood lasted for nine days and, in addition to the significant material damage in isolated villages, lost livestock, and crops, it caused two casualties, 115 injured, and about ten thousand evacuees (Loureiro, 2009). In Santarém (Ómnias hydrometric station), the maximum instantaneous flow value was estimated at 14,500 m<sup>3</sup>/s, which appears to be associated with a return period of 100 years (Amaral et al., 2022).

For the 1979 flood, the hydrograph at the river boundary was obtained by routing the hydrograph gauged at the Almourol staff (Fig. 1), 40 km upstream (<https://snirh.apambiente.pt/>). Observations from another staff gauge were available closer to that boundary, but the rating curve was only defined inside the main channel. For river flows above 2200 – 4000 m<sup>3</sup>/s (depending on the sediments accumulated in the riverbed), that rating curve is inadequate because the river spills onto the flood plain. Atmospheric pressure, significant wave height and river flow reached 998 hPa, 7 m and 15,100 m<sup>3</sup>/s, respectively.

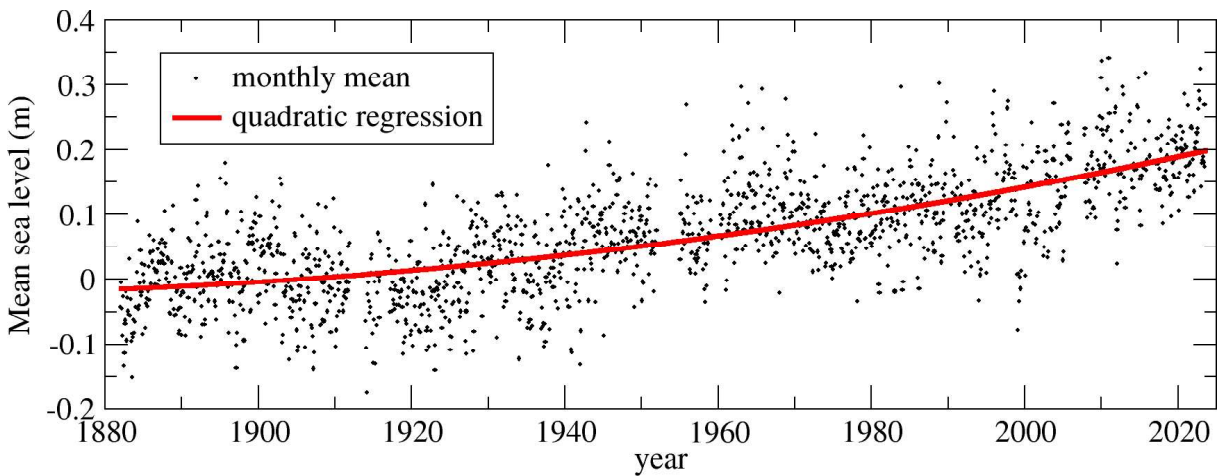


**Fig. 2.** Determination of the present mean sea level using data from the Cascais tide gauge. The reference level is determined as the average of all the data prior to 1938.

### 2.3. Model implementation and validation

A 2D implementation of the shallow water model SCHISM (Zhang et al., 2016), including its wind-wave module WWM, was used to generate inundation maps. The model domain (Fig. 3a) encompasses the entire potentially floodable area in Vila Franca de Xira municipality, extending from the ocean 90 km upstream. The grid resolution varies between less than 5 m in flood-prone areas to 1,600 m at the ocean boundary. To account for narrow dykes, a row of nodes is placed over their crests (Fig. 3b). This approach balances computational efficiency with potential minor errors due to the simplified dyke representation.

The model is forced by tides, surges, waves, atmospheric pressure, wind, and river flow (Fortunato et al., 2017). It exhibits root mean square errors of 5-20 cm for water elevations over a year (Fig. 4a). The wave component of the model was validated in operational conditions (<https://connect-portal.lnec.pt/connect/>) at a wave buoy located at the mouth of the estuary for the first semester of 2024. The following errors were obtained: root mean square errors: 35 cm (Hs) and 1.5 s (TM02); biases: 25 cm (Hs) and 0.61 s (TM02). Additionally, validation for extreme events (100-year river flood and major storm with large waves) has been conducted (Fortunato et al., 2017). Sensitivity analyses revealed that atmospheric pressure significantly impacted water levels during the river flood at Vila Franca de Xira, with offshore and local waves having a lesser influence. Past inundation events further supported the model's spatial accuracy.

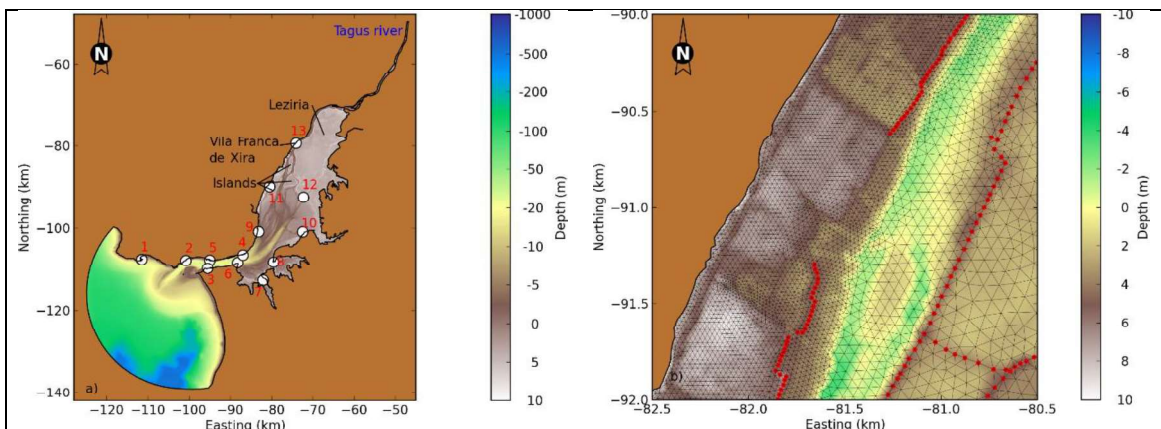


**Fig. 3.** Estuarine model domain and bathymetry: a) global view and tidal stations used in Fig. 4a; b) detail in the study region. The white circles represent the tidal stations used for validation. The red circles indicate nodes placed on the crest of the dykes.

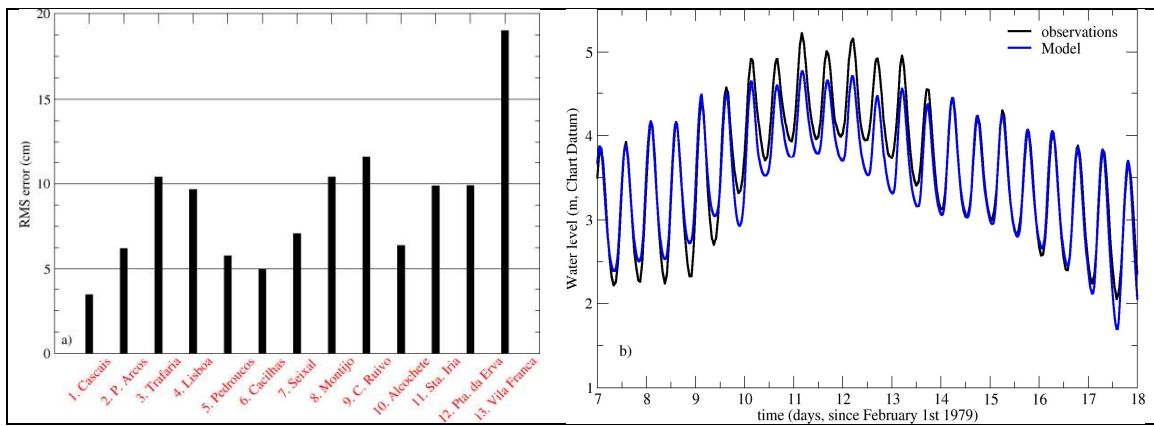


Fig. 4. Estuarine model validation: a) root mean square elevation errors for a 1972 simulation at the stations shown in Fig. 1a; b) water elevations at station 13 (Vila Franca de Xira) during the 1979 flood

### 3. Results and discussion

The inundation maps for the two extreme events and the two MSL conditions (present sea level and considering a 1.5 m sea level rise) are presented in Fig. 5.

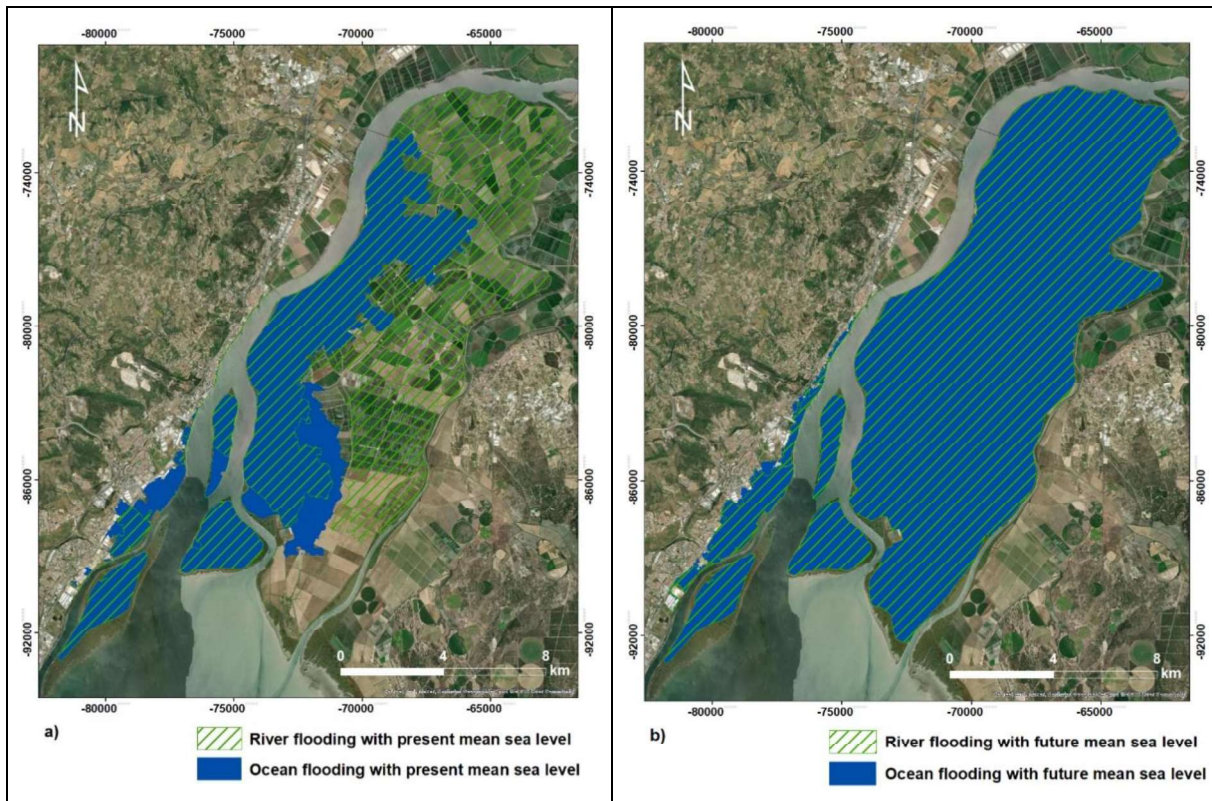


Fig. 5. Inundation of ocean and river origins in the upper Tagus Estuary for the present (a) and future (b) mean sea levels.

At present MSL, storm surge inundation covers the three islands, 15.5 km<sup>2</sup> on the left bank, and 4.1 km<sup>2</sup> on the right bank (Fig. 5a). River flooding partially inundates the agricultural area between the Tagus, Sorraia and Risco rivers (Lezíria) and the three islands, with significantly less inundation on the right bank near Vila Franca de Xira compared to the storm surge scenario.

A 1.5 m sea level rise significantly increases inundation extent, with the Lezíria and islands entirely flooded during storm surges (Fig. 5b). Extreme water levels rise from 2-3 m to about 4 m due to both the direct sea level rise and increased tidal amplification by resonance (Guerreiro et al., 2015). Oceanic flooding becomes more severe than fluvial flooding.

The behavior differs significantly between the two situations. For the present MSL, the maximum water levels grow by about 2 m landward between the limits considered. In contrast, for the future MSL this growth is very small. At the upstream limit of the Vila Franca de Xira municipality, sea level rise will even reduce the maximum water level.

The observed reduction in maximum water levels at the upstream limit with future sea level rise might seem counterintuitive. In this scenario, the inundated agricultural area between the rivers will act as a large estuary with a significantly increased cross-section. This reduces flow velocities and bed shear stress, leading to a more horizontal water surface compared to the present conditions, where the stretch behaves more like a narrow river. Specifically, the cross-section will increase significantly, which will reduce the velocities and the bottom friction. The gradients of the sea surface will decrease because the bed stress is balanced by the barotropic pressure gradient. The water surface will therefore become more horizontal than presently. This discussion assumes the present geometry remains unchanged. For example, if the dyke crest heights are increased in the future to mitigate inundation, the phenomena described above would be prevented and higher water levels would occur.

#### 4. Conclusions

This paper describes the development of inundation maps for areas vulnerable to extreme flooding from both rivers and oceans. The maps were generated using a sophisticated numerical model that incorporated all relevant forces and physical processes. The descriptions of geometry and physical processes are significantly more detailed than those used in previous generations of inundation maps in Portugal.

The results provide new insights into the potential extent of flooding during extreme events. On the left bank of the river, the extent of the inundation can be dramatic. This low-lying agricultural land is protected by dykes, which could be severely damaged by the overflow of water. An analogous situation occurred during the 2010 Xynthia storm. A more severe storm would probably damage a longer stretch of the dyke. Similarly, the three islands in the upper estuary can be inundated during extreme events from both the river and the ocean. One of them (Mouchão da Póvoa) is actually now flooded at every tidal cycle since its dyke was breached in 2016. On the right riverbank, the extent of the inundation is much smaller due to the topography. However, the consequences may be more severe because urban and industrial areas can be affected. In particular, results indicate the potential for extensive inundation of an airfield.

Despite the level of detail used in the study, several factors were identified that still limit the accuracy of the maps and constitute areas for future research.

The analysis revealed a high sensitivity of extreme water levels to river flow rates, particularly for a major flood event in 1979. However, the available data for that event consisted solely of daily average flow values. The results could potentially differ significantly if data with higher temporal resolution (instantaneous values) were incorporated.

Another limitation arose from the indirect measurement of river flow, which was calculated based on water elevation measurements. This approach introduces uncertainties during extreme events due to the need to extrapolate the stage-discharge curves.

Furthermore, during significant river floods, the velocities in the upstream reaches of the domain are very high, leading to numerical oscillations. These spurious oscillations necessitated the application of specific damping methods (e.g., high implicitness and numerical filters). While the precise impact of these oscillations and the damping techniques on model accuracy remains unclear, sensitivity analyses suggest they may be significant.

To optimize computational efficiency, dykes were represented in the grid as single rows of nodes along their crests. However, the influence of this simplification on overall accuracy requires further investigation.

The high-resolution topographic data (2 meters) employed in the study exhibited limitations in accuracy, with a root mean square error of 0.45 meters and 90% of data points falling within a 0.75-meter error margin. These errors, particularly at dyke crests, could significantly overestimate the volume of water overflowing the structures.

The estimation of the Manning friction coefficient in the estuary margins relied upon land-use maps. Due to the coarser resolution of this information compared to the model grid, friction may be poorly represented in

crucial areas. Additionally, the future evolution of land use within the estuary margins remains uncertain and was not considered.

Finally, the study acknowledges the significant uncertainty surrounding the future sea level rise. The scenario employed in the model, a 1.5-meter increase by the end of the 21st century, represents a prudent estimate based on projections from the International Panel on Climate Change.

### **Acknowledgements**

This study was funded by the Vila Franca de Xira Municipality. The 2D operational model of the Tagus estuary was implemented and validated within the CONNECT project funded by the Copernicus Marine Service National Collaboration Programme 2022-2028.

### **References**

- Amaral S, Rocha F, Viseu T (2022) Estimativa de caudais de cheias no rio Tejo. Análise estatística de caudais máximos nas estações hidrométricas de Ómnias, Almourol e Tramagal. Relatório LNEC 53/2022 (in Portuguese).
- Fortunato AB, Oliveira A, Baptista AM (1999) On the effect of tidal flats on the hydrodynamics of the Tagus estuary, *Oceanologica Acta* 22/1, 31-44
- Fortunato AB, Freire P, Bertin X, Rodrigues M, Ferreira J, Liberato ML (2017) A numerical study of the February 15, 1941 storm in the Tagus estuary, *Continental Shelf Research* 144, 50-64
- Freitas JG, Dias JA (2013) 1941 windstorm effects on the Portuguese Coast. What lessons for the future? *Journal of Coastal Research*, Special Issue 65: 714-719.
- Guerreiro M, Fortunato AB, Freire P, Rilo A, Taborda R, Freitas MC, Andrade C, Silva T, Rodrigues M, Bertin X, Azevedo A (2015) Evolution of the hydrodynamics of the Tagus estuary (Portugal) in the 21st century, *Journal of Integrated Coastal Zone Management* 15/1, 65-80
- Hersbach H, Bell B, Berrisford P, Hirahara S, Horányi A, Muñoz-Sabater J, Nicolas J, Peubey C, Radu R, Schepers D, Simmons A, Soci C, Abdalla S, Abellan X, Balsamo G, Bechtold P, Biavati G, Bidlot J, Bonavita M, Thépaut J-N (2020) The ERA5 global reanalysis, *Quarterly Journal of the Royal Meteorological Society*, 146/730, 1999-2049.
- Loureiro JM (2009) Rio Tejo: As grandes cheias 1800-2007. Tágides, Administração da Região Hidrográfica do Tejo, Comissão de Coordenação e Desenvolvimento Regional de Lisboa e Vale do Tejo, 80 pp (in Portuguese).
- Muir-Wood R (2011) The 1941 February 15th Windstorm in the Iberian Peninsula. *Trébol*, 56, 4-13.
- Zhang YJ, Ye F, Stanev EV, Grashorn S (2016) Seamless cross-scale modeling with SCHISM, *Ocean Modelling* 102, 64